1-2014

Optical Properties of Carbon Microcoils

Muneaki Hikita
University of Dayton, hikitam1@udayton.edu

Li Cao
University of Dayton, lcao01@udayton.edu

Khalid Lafdi
University of Dayton, klafdi1@udayton.edu

Optical properties of carbon microcoils

Muneaki Hikita, Li Cao,[a] and Khalid Lafdi[a]
University of Dayton, Dayton, Ohio 45469, USA

(Received 15 October 2013; accepted 15 January 2014; published online 29 January 2014)

Carbon microcoils (CMCs) have emerged as versatile material artifacts for a variety of applications due to their helical and spiral structures. Embedded in matrix, CMCs have already been demonstrated for their potential tactile/proximity sensor application. In this study, CMCs were prepared using a conventional chemical vapor deposition method, and then were functionalized with octadecylamine. Upon photoexcitation, the functionalized CMCs exhibited photoluminescence in the visible region, which has never been found before. Similar to carbon based nanoparticles, the photoluminescence of CMCs was attributed to electron-hole radiative recombination after surface passivation. The results suggested that this kind of fluorescent functionalized CMCs might be used as a promising class of optical agents for biological applications. © *2014 AIP Publishing LLC*. [http://dx.doi.org/10.1063/1.4863501]

Coiled carbon nanofibers or carbon microcoils (CMCs), as one kind of three-dimensional (3D) attractive forms due to their unique helical and spiral morphologies, exhibit remarkable mechanical, electrical, and magnetic properties.[1–3] Various practical applications based on these properties have been widely explored such as composite reinforcement, electromagnetic interference (EMI) shielding, hydrogen absorption, storage, etc.[4–9] Interestingly, the characteristic helical structure of CMCs is similar to those of DNA and some proteins,[10] and has been recently studied for potential technological applications in biology and medicine.[8,9,11] Furthermore, the broadband absorption of MHz and GHz electromagnetic waves, high electrical conductivity, and superelasticity, and also generally non-toxic behavior have made CMCs to be valuable materials for biological applications.[8,9,11] As is known, numerous Meissner corpuscles, working as tactile sensing receptors on the skin, can sense a variety of stresses or stimuli, which is very complicated biological sensing system and difficult to be mimicked with today's technologies. The various properties of CMCs might be a promising candidate to be used as high sensitive artificial sensors to mimic the behaviors of tactile corpuscles. Motojima *et al*. had investigated the biological sensor application of CMCs, and demonstrated CMCs embedded into polysilicon matrix could be used as tactile/proximity sensor for minimal access surgery (MAS), which is one kind of clinical technique developed to reduce the traumatic effect during surgical operation.[11] To conduct MAS operation, a light source to illuminate the operative sites is usually required. For easily tracking the tactile sensors during MAS, it would be much helpful if this kind of artificial biological sensors can be photoluminescent in the visible under illumination.

The optical properties of carbon based materials, especially photoluminescence emissions have attracted recent growing attention.[12,13] It has been well known that the defect-derived photoluminescence emission in carbon based nanomaterials is generally strong, and can be significantly enhanced when the defects are effectively passivated. This kind of passivation is similar to those found in nanodiamonds, carbon dots, and functionalized carbon nanotubes.[14–16] For example, Mochalin and Gogotsi reported blue fluorescent nanodiamonds with octadecylamine (ODA) functionalization for prospective bioimaging applications.[14] CMCs, usually consisting of less-ordered nanocrystalline graphite,[17,18] should possess a large amount of defects from the edges and/or oxidation sites of the graphite nanocrystallites, and therefore might have great potential to be photoluminescent with suitable excitations.

In this study, CMCs were prepared using a chemical vapor deposition (CVD) method. X-ray diffraction (XRD) result showed there were many small graphite nanocrystallites in the CMCs, which was confirmed with Raman characterization. After functionalization with ODA, these CMCs were photoluminescent in the visible region, which has never been found before. Defect passivation with polymer was considered to be responsible for the photoluminescence emission of ODA functionalized CMCs. This kind of fluorescent CMCs was demonstrated its great potential to be used as an optical marker for easily tracking purpose during MAS operation, and may pave the way as one kind of optical imaging agent for multimodality cancer detection in the future.

Thiophene (≥99%), nickel powder (5 μm in diameter), and Octadecylamine (90%) were supplied from Sigma-Aldrich; Isopropyl alcohol (99.9%), nitric acid (70%), and deionized water were purchased from Fisher Scientific; Acetylene, hydrogen, argon gases were from Airgas. Graphite substrates were purchased from Americarb. Glass microfiber filter (6 μm) was supplied from Whatman. The morphologies of samples were characterized using Hitachi S-4800 high resolution scanning electron microscope. The XRD patterns were acquired using a Rigaku Ultima III XRD diffractometer operated at 40 kV and 44 mA. The X-ray wavelength was 0.154 nm generated with a copper X-Ray tube. UV/vis absorption spectrum was recorded on a PerkinElmer Lamda 950 spectrophotometer. Fluorescence spectra were obtained on a PerkinElmer LS 55 luminescence spectrometer equipped with a high energy pulsed Xenon source. Renishaw *inVia* Raman microscope with Renishaw RL633 laser was used for the Raman scattering analysis.

[a]Authors to whom correspondence should be addressed. Electronic addresses: lcao01@udayton.edu and klafdi1@udayton.edu

Nickel powder (30 mg) as catalyst was rubbed on a 10×2 cm^2 graphite substrate, where CMCs were produced by CVD using acetylene and hydrogen with the addition of argon as a carrier gas. The flow rates of acetylene, argon, and hydrogen were 30 sccm, 40 sccm, and 70 sccm, respectively. Thiophene (C_4H_4S) as the sulfur source, bubbled at 23 °C with hydrogen gas (3 sccm), was introduced into a quartz tube (3.4 cm in diameter). The samples were collected after 1.5 h reaction at ~700 °C.[19]

To functionalize CMCs, the obtained sample (50 mg) was sonicated in nitric acid at room temperature for 1 h, and subsequently heated with home-made microwave oven (600 W) reflux system for 0.5 h. Upon acid treatment, CMCs dispersed in acid solution were filtrated, and after that was washed with deionized water for 6 times and then with isopropyl alcohol for 2 times. Following dried in air at room temperature, the resultant solid sample was mixed thoroughly with prepared ODA/isopropyl alcohol solution (50 mg/mL), and then the mixed solution was boiled using microwave oven reflux system for 60 h under nitrogen gas protection. After cooled to room temperature, dark brown solution in isopropyl alcohol was obtained, and then centrifuged (3000 rcf) using isopropyl alcohol solvent for ten times to remove extra ODA. The final residue was collected and dried in air at room temperature, and then redispersed into isopropyl alcohol solvent for optical characterization.

A portion of the as-produced CMCs without functionalization was placed on an electrical conductive tape for scanning electron microscopy (SEM) analysis. As shown in Figure 1, CMCs were made up of uniform double-helix morphology. The average external coil diameter was about 2.5 μm and the average nanofiber diameter was about 870 nm. As discussed in the literature,[19] sulfur compounds were critical for the synthesis of coil structure. For example, Chen and Motojima had discussed the morphologies and dimensions of CMCs were strongly affected by the anisotropy of carbon deposition and also Ni-C-S composition due to the change of thiophene content in the reaction, and suggested CMCs with smaller diameters could be produced with lower content of thiophene vapors carried in the gas flow.[20] Some other factors, such as reaction temperature, reaction time, substrates, and catalysts, also played important roles for the coil morphologies, which had been discussed in the literature.[19,20]

Powder XRD is a widely used characterization technique for identification of specimen and determination of

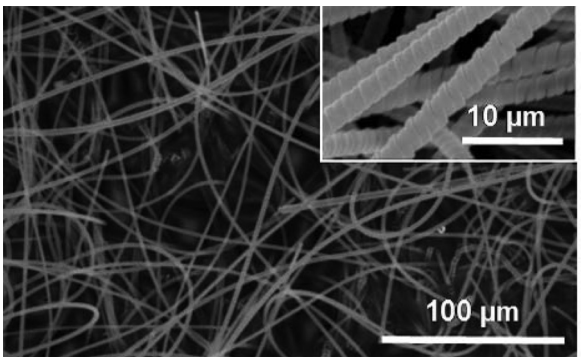

FIG. 1. SEM image of CMCs. High magnification SEM image of CMCs is shown in the inset.

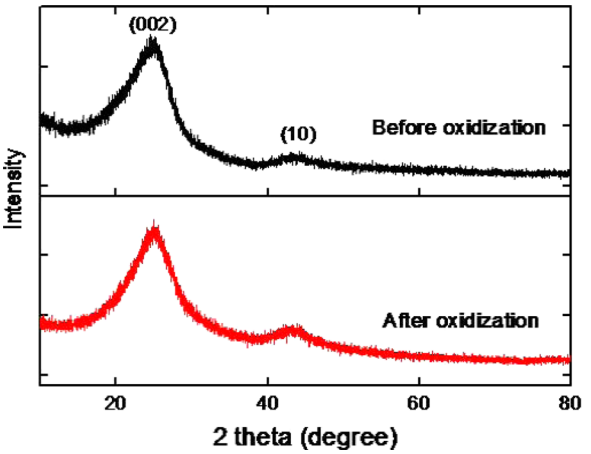

FIG. 2. XRD patterns of CMCs before (black curve) and after (red curve) oxidation.

crystal structure. Shown in Figure 2, XRD pattern of as-produced CMCs illustrated two distinct characteristic peaks: 25.2° and 43.3° with full width at half maximum (FWHM) were 6.2° and 5.6°, respectively. The first peak is related to the (002) plane of graphite with interlayer spacing of ~0.34 nm, and the second broad peak is ascribed to the (10) band which comes from both (100) and (101) peak of graphitic structure as discussed by other groups.[21,22] In comparison, oxidized CMCs also showed similar two peaks (Figure 2), but their FWHMs were slightly broader than those of as-produced CMCs. For example, the (002) peak of oxidized CMCs was 0.3° broader than as-produced CMCs. Based on (002) and (10) peaks of CMCs, the graphitic crystalline sizes can be calculated with Scherrer's equation. The equation for graphite structure is described as[22–24]

$$L_a = \frac{1.84\lambda}{B\cos\theta_B}, \tag{1}$$

$$L_c = \frac{0.9\lambda}{C\cos\theta_C}, \tag{2}$$

where λ is the wavelength of X-ray source (0.154 nm). Correspondingly, L_a or L_c is the crystalline size parallel or perpendicular to basal plane, B or C represents FWHM in radians of the (10) or (002) peak, θ_B or θ_C is the Bragg angle of (10) or (002) peak. The broadness of the two peaks is attributed to the small size of graphitic crystallites, also called graphite nanoparticles or graphite quantum dots. According to the calculation, the crystalline sizes of L_a and L_c for as-produced CMCs were 3.62 nm and 1.32 nm. The calculated results suggested the possible presence of amorphous carbon and disordered small graphite nanocrystallites in the growth of CMCs, which is similar with the previous report in the literature.[17,18] After the acid treatment, the calculated slightly broader FWHM of the (002) peak of oxidized CMCs compared to as-produced ones indicated the size of graphite nanocrystallites became a little smaller in oxidized CMCs. It is rational that acid oxidation may help to cut graphite nanoparticle into smaller ones, as generally reported in the literature.[25] Our XRD results proved that oxidation occurred during acid treatment, and this kind of oxidation was not only for generation of carboxylic (COOH)

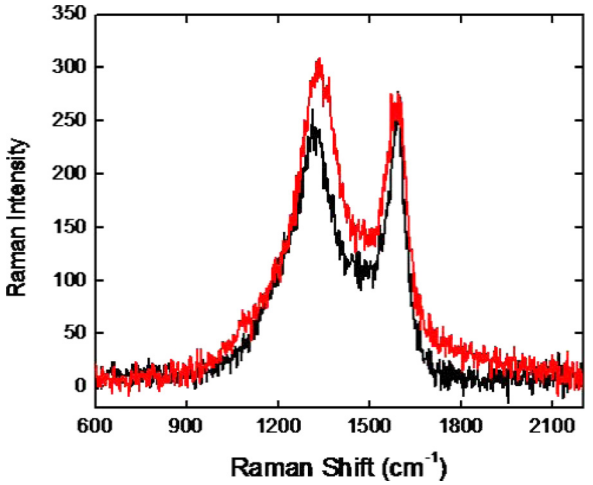

FIG. 3. Raman spectra of CMCs (black curve) and oxidized CMCs (red curve).

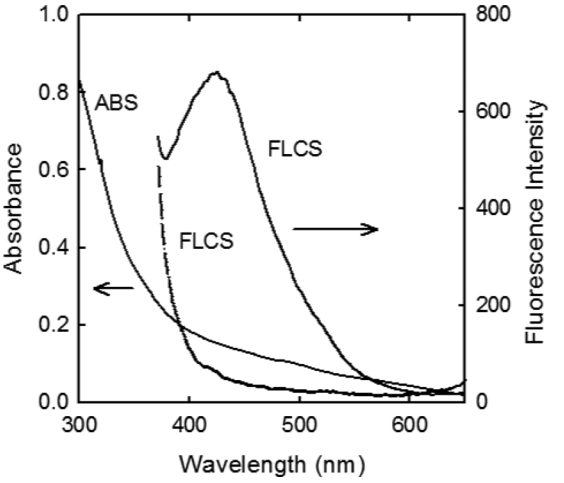

FIG. 4. UV/vis absorption (ABS) and fluorescence emission (FLSC, 350 nm excitation) spectra of ODA functionalized CMCs in isopropyl alcohol (solid curves). As also shown for the comparison, the acid treated CMCs but without ODA were not emissive (dashed curve).

groups,[26] but creating defects and pits within coherent crystallite zone of CMCs.[25] To further check this point, Raman scattering characterization was conducted under Raman microscopy system equipped with He-Ne laser.

Raman spectroscopy has been used as one type of non-destructive techniques for characterization of the lattice vibration modes of carbon-base materials.[27] In general, there are two prominent features in the Raman spectra of carbon based materials, so called G and D bands, which are from E_{2g} optical phonon mode that involves in-plane sp^2 bond stretching of the graphite lattice and disorder-induced mode, respectively. Based on the ratio between G and D peaks, Raman scattering results can generally indicate the quality, crystalline size, or defect density of carbon based materials.[27,28] Figure 3 showed the comparison of Raman scattering of CMCs before (black curve) and after (red curve) oxidation with nitric acid. The incident laser excitation wavelength is 633 nm. Prior to oxidation, the peaks of D band and G band are $\sim$1323 cm^{-1} and $\sim$1594 cm^{-1}, and then shifted to $\sim$1335 cm^{-1} and $\sim$1595 cm^{-1} correspondingly after oxidation. The ratio of $I_D : I_G$ for oxidized CMCs is larger ($I_D : I_G \sim 1.1$) compared to non-oxidized CMCs ($I_D : I_G \sim 0.9$), indicating more defects were generated during nitric acid treatment.[29,30] Based on the empirical Tuinstra-Koenig relationship that the size of small graphite nanocrystallites (sp^2 cluster) was inversely proportional to that the ratio of $I_D : I_G$,[31,32] the average crystalline size parallel to basal plane (L_a) for CMCs was about 4 nm., which was close to the XRD result. After acid oxidation, the increase of the ratio of $I_D : I_G$ indicated the size of the small graphite crystallites decreased, which was reasonable because of the cutting of graphite nanocrystallites during oxidation.[25] These results were consistent with the XRD analysis conclusion. Due to the large diameter of carbon nanofiber ($\sim$870 nm) of CMCs, it was not easy for the nitric acid solution to oxidize CMCs completely when heated in microwave for only 30 min, which means many defects were most likely created on the surface of CMCs. In addition, the blue shift ($\sim$12 cm^{-1}) of the Raman peak of D band after acid treatment confirmed the oxidation process for the CMCs.[25] Similar to oxidation of carbon nanomaterials,[25] the acid treatment created COOH groups on the surface of CMCs and provided the platform for following functionalization.

As is known, ODA functionalized carbon nanoparticles are photoluminescent due to the defect passivation.[14] In this experiment, ODA was dissolved in isopropyl alcohol and heated for 60 h using a home-made microwave oven reflux system for functionalization under nitrogen protection. Dark brown ODA-functionalized CMCs solution was obtained and washed for absorption and photoluminescence characterization.

After washed with isopropyl alcohol, ODA functionalized CMCs were redispersed in isopropyl alcohol and characterized using UV/vis absorption and fluorescence spectrophotometers. As shown in Figure 4, there was no obvious feature in the absorption spectrum of ODA functionalized CMCs. The photoluminescence spectrum indicated ODA functionalized CMCs were fluorescent in the visible. For comparison, CMCs before functionalization were measured but no fluorescence was observed. The emission peak for the functionalized CMCs was about 423 nm at 350 nm excitation. As were proved with XRD and Raman results, the prepared CMCs using the CVD method were not well crystalline. They were made of turbostratic carbons (disordered carbons) with small crystalline nanoparticles ($\sim$1–2 nm in thickness and $\sim$3–4 nm in lateral size). These small nanocrystallites were localized in the CMCs, and therefore behaved like embedded carbon nanoparticles or so called graphite nanoparticles. Further, oxidation process not only increased the defective level but also decreased (cutting) the size of graphite nanocrystallites. During chemical functionalization, some of small nanocrystallites located on the surface of CMCs were passivated preferentially at their defect sites, and thus generated photoluminescence when excited with suitable wavelength. Stability study of the fluorescent CMCs was conducted and showed there was nearly no change for 30 days. Further, investigation on the fluorescent CMCs is needed and planned. The fluorescence property of functionalized CMC may serve as a highly promising platform for the biological optical tracking applications in the future.

Mechanistically, radiative recombinations of electrons and holes confined on the small nanoparticle surface are responsible for the observed blue fluorescence. The electrons and holes are generated likely due to efficient photoinduced charge separations in the graphite nanoparticles in the CMCs, and the role of the surface passivation by the ODA functionalization is probably to make the surface sites more stable to facilitate more effective radiative recombinations.[12]

In summary, CMCs were grown on a graphite substrate using a conventional CVD method. X-ray diffraction and Raman characterization demonstrated these CMCs consisted of small graphite nanocrystallites. Further, oxidation with nitride acid decreased the size of these small nanocrystallites and generated more defects as well on their surface or edges. The oxidized CMCs were passivated with ODA, and became fluorescent in the visible region after photoexcitation. Similar to passivated carbon-based nanoparticles, this kind of photoluminescence was mechanistically attributed to radiative recombinations of surface confined electrons and holes in the small graphite nanocrystallites in the CMCs. The fluorescent CMCs may serve as a promising tool for the optical tracking agent during MAS operation or an optical multimodality imaging agent for cancer detection.

This work has been supported in part by the University of Dayton Office for Graduate Academic Affairs through the Graduate Student Summer Fellowship Program.

[1]K. Kaneto, M. Tsuruta, and S. Motojima, Synth. Met. **103**(1), 2578–2579 (1999).
[2]Z. Tianliang, W. Yuehong, Z. Kuangyu, L. Qian, and T. Ye, Chin. J. Aeronaut. **20**(6), 559–563 (2007).
[3]N.-K. Chang and S.-H. Chang, IEEE Trans. Nanotechnol. **7**(2), 197–201 (2008).
[4]X. Chen, S. Yang, and S. Motojima, Mater. Lett. **57**(1), 48–54 (2002).
[5]Y. Kato, N. Adachi, T. Okuda, T. Yoshida, S. Motojima, and T. Tsuda, Jpn. J. Appl. Phys., Part 1 **42**, 5035–5037 (2003).
[6]S. Motojima, X. Chen, S. Yang, and M. Hasegawa, Diamond Relat. Mater. **13**(11), 1989–1992 (2004).
[7]T. Katsuno, X. Chen, S. Yang, and S. Motojima, Diamond Relat. Mater. **16**(4), 1000–1003 (2007).
[8]K. Yoshimura, K. Nakano, T. Miyake, Y. Hishikawa, C. Kuzuya, T. Katsuno, and S. Motojima, Carbon **45**(10), 1997–2003 (2007).
[9]K. Yamauchi, T. Imada, and T. Asakura, J. Phys. Chem. B **109**(37), 17689–17692 (2005).
[10]C. Kuzuya, M. Kohda, Y. Hishikawa, and S. Motojima, Carbon **40**(11), 1991–2001 (2002).
[11]S. Yang, X. Chen, H. Aoki, and S. Motojima, Smart Mater. Struct. **15**(3), 687–694 (2006).
[12]L. Cao, M. J. Meziani, S. Sahu, and Y.-P. Sun, Acc. Chem. Res. **46**(1), 171–180 (2013).
[13]L. Cao, S. Sahu, P. Anilkumar, C. Y. Kong, and Y.-P. Sun, MRS Bull. **37**(12), 1283–1289 (2012).
[14]V. N. Mochalin and Y. Gogotsi, J. Am. Chem. Soc. **131**(13), 4594–4595 (2009).
[15]C. Liu, P. Zhang, F. Tian, W. Li, F. Li, and W. Liu, J. Mater. Chem. **21**(35), 13163–13167 (2011).
[16]X. Wang, L. Cao, C. E. Bunker, M. J. Meziani, F. Lu, E. A. Guliants, and Y.-P. Sun, J. Phys. Chem. C **114**(49), 20941–20946 (2010).
[17]H. Bi, K. Kou, A. Rider, K. Ostrikov, H. Wu, and Z. Wang, Appl. Surf. Sci. **255**(15), 6888–6893 (2009).
[18]Y. Furuya, T. Hashishin, H. Iwanaga, S. Motojima, and Y. Hishikawa, Carbon **42**(2), 331–335 (2004).
[19]S. Motojima, Y. Itoh, S. Asakura, and H. Iwanaga, J. Mater. Sci. **30**(20), 5049–5055 (1995).
[20]X. Chen and S. Motojima, J. Mater. Sci. **34**(22), 5519–5524 (1999).
[21]A. Cuesta, P. Dhamelincourt, J. Laureyns, A. Martinez-Alonso, and J. M. Tascón, J. Mater. Chem. **8**(12), 2875–2879 (1998).
[22]A. Dandekar, R. Baker, and M. Vannice, Carbon **36**(12), 1821–1831 (1998).
[23]A. Sharma, T. Kyotani, and A. Tomita, Carbon **38**(14), 1977–1984 (2000).
[24]A. K. Kercher and D. C. Nagle, Carbon **41**(1), 15–27 (2003).
[25]D. Pan, L. Guo, J. Zhang, C. Xi, Q. Xue, H. Huang, J. Li, Z. Zhang, W. Yu, and Z. Chen, J. Mater. Chem. **22**(8), 3314–3318 (2012).
[26]V. Datsyuk, M. Kalyva, K. Papagelis, J. Parthenios, D. Tasis, A. Siokou, I. Kallitsis, and C. Galiotis, Carbon **46**(6), 833–840 (2008).
[27]A. Ferrari and J. Robertson, Phys. Rev. B **61**(20), 14095–14107 (2000).
[28]A. Cuesta, P. Dhamelincourt, J. Laureyns, A. Martinez-Alonso, and J. D. Tascón, Carbon **32**(8), 1523–1532 (1994).
[29]F.-H. Ko, C.-Y. Lee, C.-J. Ko, and T.-C. Chu, Carbon **43**(4), 727–733 (2005).
[30]A. Rodríguez-Fortea, M. Iannuzzi, and M. Parrinello, J. Phys. Chem. C **111**(5), 2251–2258 (2007).
[31]F. Tuinstra and J. L. Koenig, J. Chem. Phys. **53**, 1126–1130 (1970).
[32]F. Tuinstra and J. L. Koenig, J. Compos. Mater. **4**, 492–499 (1970).